

Measurement of fracture toughness and interfacial shear strength of hard and brittle Cr coating on ductile steel substrate

B.-Q. Yang^{*1,2,3}, K. Zhang², G.-N. Chen², G.-X. Luo² and J.-H. Xiao²

The fracture toughness and interfacial adhesion properties of a coating on its substrate are considered to be crucial intrinsic parameters determining performance and reliability of coating–substrate system. In this work, the fracture toughness and interfacial shear strength of a hard and brittle Cr coating on a normal medium carbon steel substrate were investigated by means of a tensile test. The normal medium carbon steel substrate electroplated with a hard and brittle Cr coating was quasi-statically stretched to induce an array of parallel cracks in the coating. An optical microscope was used to observe the cracking of the coating and the interfacial decohesion between the coating and the substrate during the loading. It was found that the cracking of the coating initiated at critical strain, and then the number of the cracks of the coating per unit axial distance increased with the increase in the tensile strain. At another critical strain, the number of the cracks of the coating became saturated, i.e. the number of cracks per unit axial distance became a constant after this critical strain. Based on the experiment result, the fracture toughness of the brittle coating can be determined using a mechanical model. Interestingly, even when the whole specimen fractured completely under an extreme strain of the substrate, the interfacial decohesion or buckling of the coating on its substrate was completely absent. The test result is different from that appeared in the literature though the identical test method and the brittle coating/ductile metal substrate system are taken. It was found that this difference can be attributed to an important mechanism that the Cr coating on the steel substrate has a good adhesion, and the ultimate interfacial shear strength between the Cr coating and the steel substrate has exceeded the maximum shear flow strength level of the steel substrate. This result also indicates that the maximum shear flow strength level of the ductile steel substrate can be only taken as a lower bound estimate on the ultimate shear strength of the interface. This estimation of the ultimate interfacial shear strength is consistent with the theoretical analysis and prediction presented in the literature.

Keywords: Hard and brittle coating, Fracture toughness, Ductile steel substrate, Interfacial shear strength, Tensile test

Introduction

Hard and brittle coatings bonded to ductile substrates have many diverse applications, such as in wear-resistant coatings, anticorrosion protective coatings and thermal barrier coatings.^{1–5} Field observations as well as laboratory test results indicate that the typical failure

mode of such coating–substrate systems often is a two stage process:

- (i) the first stage is that when a coating–substrate system is under sufficient tensile stress it becomes energetically favourable for through thickness cracks to develop in the coating
- (ii) the second stage is that when the crack tip reaches the interface and the crack can propagate along the interface or into the substrate.^{6–9} The propagation of the crack along the interface can lead to the spallation or loss of the coating from the substrate.

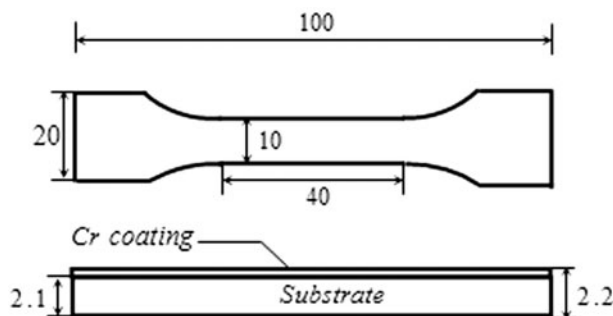
Thus, the fracture and interfacial adhesion properties of the coating on its substrate are considered to be crucial intrinsic parameters determining performance and

¹Division of Engineering Mechanics, Department of Mechanical Engineering, Armored Force Engineering Institute, No. 21, Du Jia Kan, Chang Xin Dian, Beijing 100072, China

²Laboratory of surface modification, Institute of mechanics, Chinese Academy of Sciences, No. 15 Bei si huan xi Road, Beijing 100080, China

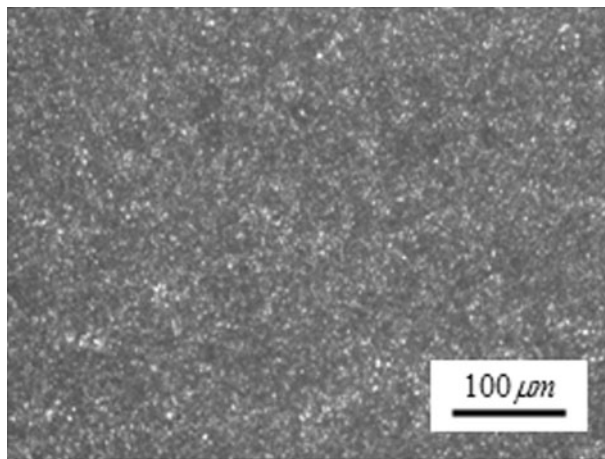
³Graduate School of the Chinese Academy of Sciences, Beijing 100080, China

*Corresponding author, email yangbq1022@tom.com



1 Schematic illustration of dimensions of specimen

reliability of coating–substrate system. In this work, two important mechanical properties of the coating–substrate system, i.e. the fracture toughness of the coating and the interfacial shear strength between the coating and substrate were investigated. The higher fracture toughness means a higher crack propagation resistance, and the higher interfacial shear adhesive strength means a higher crack initiation resistance during the shear stress loading. Various experimental methods such as the pull-off test,^{10,11} scratch test,^{12–15} indentation test,^{14–19} impact test^{20,21} and laser ultrasonic testing method^{22,23} have been used to evaluate the coating fracture properties and interfacial adhesion properties between the coating and the substrate. However, the methods mentioned above for adhesion measurement have limitations. For example, for the pull-off test, the adhesive used to glue a sample to the sample holder is required to have its adhesive strength higher than that of the interface. Generally, this test is suitable for the measurement of an adhesive strength that is weaker than 90 MPa.¹⁵ For the scratch test, a small diamond tip moves over the thin hard coating surface under a progressively increasing load. The initiation of interfacial decohesion is detected from acoustic emission signals or the load–displacement curve. The critical load corresponding to the initiation of interfacial decohesion is used to evaluate the adhesion. However, the test is influenced by a number of intrinsic and extrinsic factors that are not adhesion related and the results of the test are usually regarded as only semiquantitative.¹² It should be noticed that, for a brittle coating on a ductile metal substrate, the uniaxial tensile test has been adopted to evaluate the mechanical properties of the coating–substrate material system in some recent investigations.^{7,24–30} Xie and Wei⁷ stated, like any other type of mechanical tests, the interpretation of the uniaxial tensile test data to extract intrinsic interfacial mechanical properties of the coating attached to a substrate is still non-trivial. A tensile test not only requires a relatively simple and inexpensive testing instrument, but also can produce in a well controlled manner a large array of parallel cracks over the nominally homogeneously deformed ductile substrate and allow *in situ* observation of cracking and decohesion of the coating via various microscopy tools.⁷ Also, for this test, Ogwu *et al.*²⁴ presented fitting probability distribution functions to saturation crack spacing distribution for thin films and coatings. In this work, the uniaxial tensile test was adopted to investigate the fracture toughness and interfacial shear adhesive strength of a hard and brittle Cr coating on a normal medium carbon steel substrate.



2 Initial optical microscopy image of surface of Cr coating on steel substrate

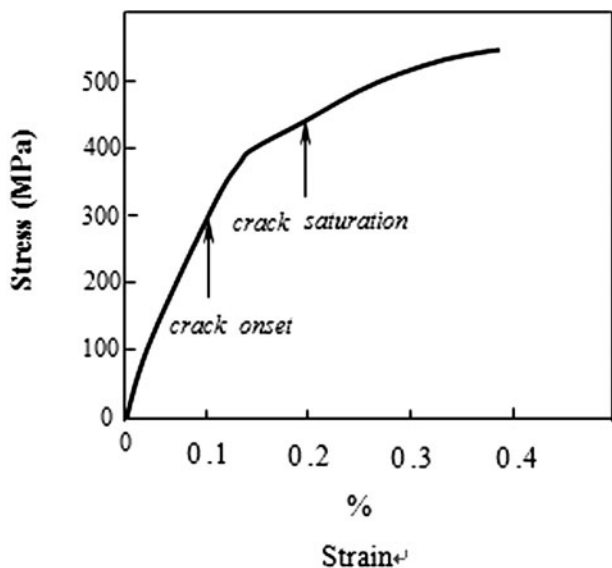
Experimental

Uniaxial tensile experiments of normal medium carbon steel electroplated with a hard and brittle Cr coating were performed in this study. The chromium coatings, composed of low contraction (LC) and high contraction (HC) chromium, were prepared by the commercial electroplating of practical chromium coated parts. The LC Cr layer $\sim 20 \mu\text{m}$ thick was predeposited as an interlayer with the commercial plating bath of chromic acid (250 g L^{-1}) and sulphuric acid (2.5 g L^{-1}), at a temperature of 85°C and a current density of 60 A dm^{-2} . The HC Cr plate approximately $80 \mu\text{m}$ thick was deposited at a lower bath temperature and a lower current density. The gage section of the dog bone shaped specimen has dimensions of 100 mm long, 20 mm wide and 2.2 mm thick while the thickness of the Cr coating was $100 \mu\text{m}$, as schematically illustrated in Fig. 1.

The cross-sectional surface of the specimen was polished to avoid stress concentration during the loading. The rate of the crosshead displacement was 0.5 mm min^{-1} . The optical microscope can be adjusted to observe the coating surface or cross-sectional surface image of the specimen. An optical metallograph of the initial surface of the Cr coating on its substrate is shown in Fig. 2.

Tensile testing of the specimen was carried out quasi-statically on a universal test setup for a coating–substrate system. Tensile loads were applied at the two ends of the specimen. After a certain displacement increment, the test was interrupted to observe whether the cracking of the coating or the interfacial decohesion occurred or not using an optical microscope. The curve of the stress versus strain derived from the test is shown in Fig. 3.

In Fig. 3, there are two significant points that should be considered: the critical strain at which the crack was initiated, and the strain at which the crack density became saturated, i.e. the number of cracks per unit axial distance became a constant after this critical strain. In this experiment, the strain at which the crack initiated is $\sim 0.1\%$, and the strain at which the crack density became saturated is $\sim 0.2\%$. Although the cracks of the coating became saturated, the specimen was still strained increasingly. Interestingly, even when the specimen



3 Curve of stress versus strain

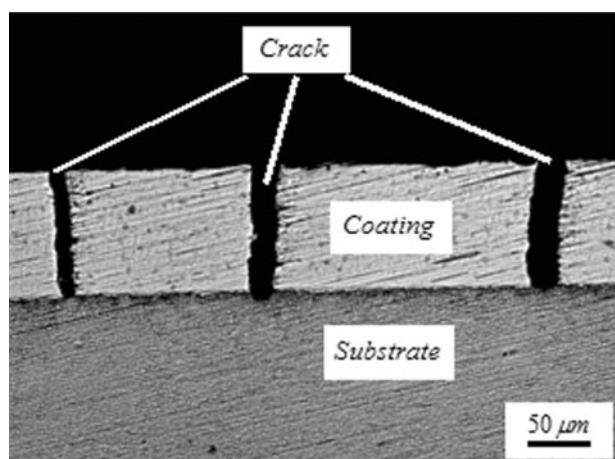
fractured completely, throughout the parallel length of the specimen under a critical strain, no interfacial decohesion or buckling of the coating could be observed, and only the quasi-periodic and through thickness cracks of the coating existed, as shown in Fig. 4. The corresponding optical micrograph of the Cr coating surface is shown in Fig. 5.

An optical micrograph of the cracking, which is characteristic of the Cr coating surface involving the fracture profile is shown in Fig. 6, in which the arrows indicate the fracture profile. From Fig. 6, it can be seen that no Cr coating peels from the substrate. Most cracks in the coating were oriented perpendicular to the tensile direction. The fact that the deflection of the cracks of the coating in Fig. 6 occurred can be attributed to the heterogeneous deformation and initial surface defects in the Cr coating.

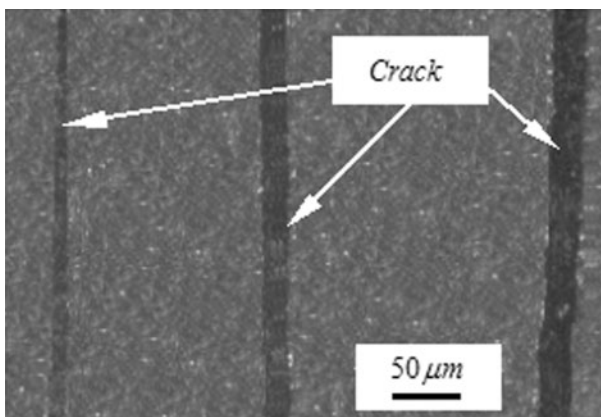
Results and discussion

Determination of fracture toughness

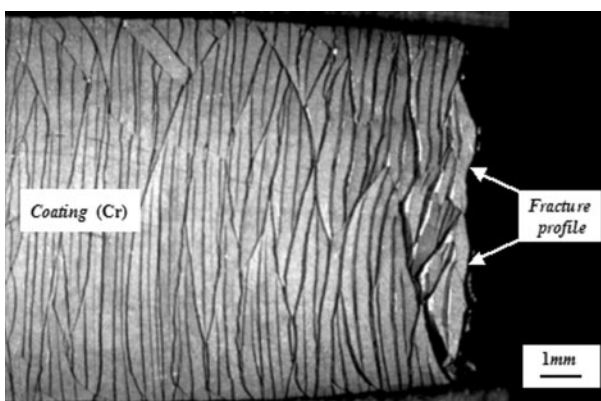
In this work, it is assumed that the brittle coating only exhibits elastic deformation and that the plastic deformation can be ignored. As mentioned above, there are two significant points in the stress versus strain curve



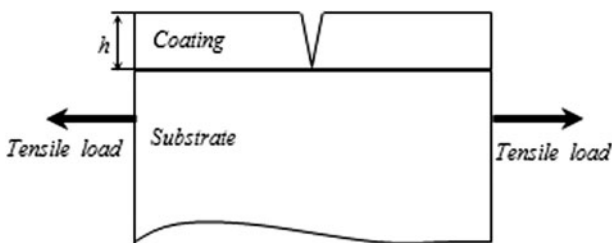
4 Cross-section optical micrograph of fractured specimen



5 Coating surface optical micrograph corresponding to cross-section optical micrograph in Fig. 4



6 Optical micrograph of Cr coating surface of fractured specimen

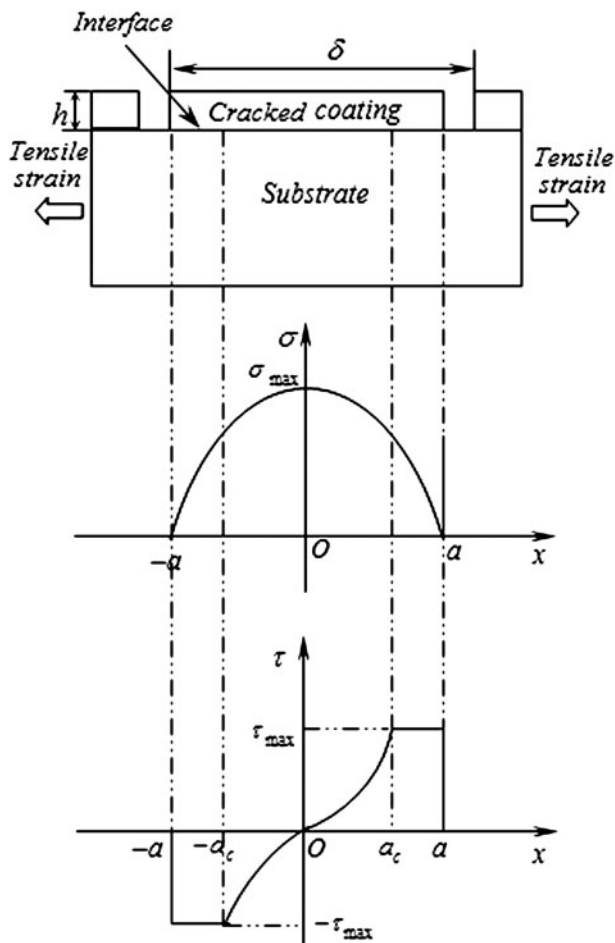


7 Mechanical model

that should be considered. One is the critical strain at which a crack of the coating is initiated. At this critical strain, the substrate still shows elastic behaviour. It should be noticed that, before this critical strain, the elastic deformation of the coating and substrate must satisfy the deformation compatibility condition, i.e. they must share the same strain. Once the crack initiates, a mechanical model is developed, as shown in Fig. 7. The fracture stress σ_c of the coating can be determined by

$$\sigma_c = E_c \varepsilon_c \tag{1}$$

E_c is the Young's modulus of the coating, and $E_c = 280$ GPa for Cr.³¹ ε_c is $\sim 0.1\%$ in this work. Therefore, the fracture stress σ_c can be calculated and it is equal to 280 MPa. Once the fracture stress is determined, the fracture toughness in terms of critical energy release rate of the coating can be calculated from³²



8 Stresses distribution characteristic in cracked coating segment and in interface with assumption of elastic-perfectly plastic model

$$G_c = \frac{1}{2} \frac{\sigma_c^2 h}{E_c} \pi g(\alpha, \beta) \tag{2}$$

where h is the thickness of the coating, and $g(\alpha, \beta)$ is a dimensionless coefficient that depends the Dundurs parameters α and β .³³ For plane strain problems, α and β are

$$\alpha = \frac{\bar{E}_c - \bar{E}_s}{\bar{E}_c + \bar{E}_s}, \beta = \frac{G_{co}(1 - 2\nu_s) - G_{su}(1 - 2\nu_c)}{2G_{co}(1 - \nu_s) + 2G_{su}(1 - \nu_c)}$$

where $\bar{E}_c = E_c / (1 - \nu_c^2)$ and $\bar{E}_s = E_s / (1 - \nu_s^2)$. E_c , G_{co} and ν_c are the Young's modulus, shear modulus and Poisson ratio of the coating respectively. E_s , G_{su} and ν_s are the Young's modulus, shear modulus and Poisson ratio of the substrate respectively. In this work, $E_c = 280$ GPa, $G_{co} = 115$ GPa and $\nu_c = 0.22$ for Cr.³¹ $E_s = 210$ GPa, $G_{su} = 82$ GPa and $\nu_s = 0.28$. Based on these given conditions, α and β can be calculated and the dimensionless coefficient $g(\alpha, \beta)$ can be given as³²

$$g(\alpha, \beta) \approx 1.38$$

So the fracture toughness of the coating can be calculated and the result is

$$G_c \approx 57.7 (\text{J m}^{-2})$$

Based on the relationship between the fracture toughness in terms of the critical energy release rate G_c and the fracture toughness in terms of the critical stress intensity

factor $K_{Ic} (G_c = K_{Ic}^2 / E_c)$, the fracture toughness G_c presented in this work is within the range of the fracture toughness of chromium described elsewhere.³¹

Estimate of interfacial shear strength

In this work, a mechanical model consisting of a two layer system is considered, as illustrated in Fig. 8, in which δ is the intercrack spacing, and a is the half length of the cracked coating segment attached to the substrate. The substrate is much thicker than the brittle coating and therefore carries almost all the applied load. Therefore, the influence of the cracking on the stress distribution in the substrate can be neglected. When the tensile strain is applied to the substrate, the shear stresses are developed in the interface or in the vicinity of the interface, resulting from the difference in Young's modulus between the coating and the substrate. The interface is assumed to be elastic-perfectly plastic in this study. As shown in Fig. 8, the maximum tensile stress occurs in the middle point of each cracked coating segment, and it vanishes at both ends of the intercrack spacing of the cracked coating segment. Also, the interfacial shear stress equals zero at the middle point and at both ends of the intercrack spacing of the cracked coating segment, and the authors assume when $a_c \leq x < a$ or $-a < x \leq -a_c$, the interface exhibits the elastic-perfectly plastic behaviour. Therefore the maximum interfacial shear stress exists in $a_c \leq x < a$ or $-a < x \leq -a_c$. Once the accumulated shear stress transferred by the interface enables the tensile stress in the coating to reach the fracture strength level, the brittle coating on the ductile substrate cracks. Based on the equilibrium condition, the relationship between the maximum tensile stress in the middle point of each cracked coating segment and the interfacial shear stress is

$$\sigma = \frac{1}{h} \int_0^a \tau(x) dx \tag{3}$$

One tensile experiment was performed by Agrawal and Raj²⁶ to evaluate the interfacial shear strength between the Si film and the copper substrate. The interfacial shear strength can be calculated from²⁶

$$\tau_b = \frac{\pi \sigma_c h}{\delta_{max}} \tag{4}$$

where, h is the thickness of the coating and it equals to 100 μm . δ_{max} is the maximum intercrack spacing when the crack density of the coating becomes saturated, and it approximately equals to 290 μm in this experiment. σ_c is the fracture stress of the coating and is equal to 280 MPa. Therefore, the interfacial shear strength can be calculated and it approximately equals to 303.2 MPa.

Another tensile experiment was conducted by McGuigan *et al.* to investigate the fracture behaviour of the glass film on the polymer substrate. At a large strain of the ductile substrate, the interfacial shear strength can be calculated from³⁰

$$\tau = 2\rho h \sigma_c \tag{5}$$

where ρ is the average crack saturation density of the coating, and is nearly equals to 5.5 mm^{-1} in this work. Base on the above conditions, the interfacial shear

strength can also be calculated and it equals to 308 MPa.

It has been found that the difference between the two interfacial shear strengths can be neglected. In this experiment, the interfacial decohesion or buckling of the coating was completely absent even when the whole specimen fractured under an extreme strain.

This experimental result is different from that described elsewhere,^{7,24–29} although identical test methods and a brittle coating–ductile metal substrate system are used. During those tests,^{7,24–29} when the crack density of the coating reached the saturation state, decohesion and the buckling of the brittle coating could be obviously observed. This situation shows that the hard and brittle Cr coating has good adhesion on this medium carbon steel substrate, and the interfacial shear strengths obtained from equations (4) and (5) can only be taken as a conservative measure to characterise the interfacial adhesion property of this material system.

In fact, the absence of decohesion and buckling of the Cr coating on its substrate in this work, can be attributed to an important mechanism that the ultimate interfacial shear strength of the Cr coating on its substrate has exceeded the maximum shear flow strength of the steel substrate. In this experiment, the ultimate elongation of the specimen under the extreme tensile strain can reach ~15%. This indicates that the ductile substrate has undergone large plastic deformation. During the fully plastic deformation, the maximum shear flow strength of the substrate can be exerted along the interface between the coating and the substrate. Because the interfacial decohesion is completely absent under the maximum shear flow stress of the substrate, the maximum shear flow strength level of the ductile steel substrate can only serve as a lower bound estimate on the ultimate shear strength of the interface. This result is also consistent with a theoretical analysis and prediction presented in Ref. 7. The tensile strength of the standard medium carbon steel substrate used in this work is 540 MPa. According to the von Mises isotropic plasticity approach, the shear strength of the substrate is only $1/3^{1/2}$ of the tensile normal strength of the substrate. Therefore, the authors can calculate the shear strength of the substrate, and it is nearly 311.8 MPa. It should be emphasised that this value only serves as a lower boundary estimate of the ultimate shear strength of the interface. From this result, it can be seen also that the interfacial shear strengths obtained from equations (4) and (5) are of the same order of magnitude as that of the maximum shear flow strength of the substrate, though they are taken as conservative values to characterise the interfacial adhesion property of this material system.

Conclusions

The fracture toughness and interfacial shear strength of a hard and brittle Cr coating on a normal medium carbon steel substrate were investigated by means of a tensile test. The results presented in this work show that

the fracture toughness of the Cr coating can be determined using a mechanical model. And interestingly, it is found that the Cr coating has a good adhesion on the steel substrate, and the maximum shear flow strength level of the ductile steel substrate can only serve as a lower boundary estimate of the ultimate shear strength of the interface.

Acknowledgement

The authors deeply appreciate the support of the National Natural Science Foundation of China (grant nos. 50531060, 50471087).

References

1. S. Sopok, C. Rickard and S. Dunn: *Wear*, 2005, **258**, 659–670.
2. J. H. Underwood, M. D. Witherell, S. Sopok, J. C. McNeil, C. P. Mulligan and G. N. Vigilante: *Wear*, 2004, **257**, 992–998.
3. P. J. Cote and C. Rickard: *Wear*, 2000, **241**, 17–25.
4. Y. A. Zhou, T. Tonomori, A. Yoshida, L. Liu, G. Bignall and T. Hashida: *Surf. Coat. Technol.*, 2002, **157**, 118–127.
5. M. H. Li, X. F. Sun, W. Y. Hu and H. R. Guan: *Surf. Coat. Technol.*, 2006, **200**, 3770–3774.
6. G. A. Smith, N. Jennett and J. Housden: *Surf. Coat. Technol.*, 2005, **197**, 336–344.
7. C. J. Xie and T. Wei: *Acta Mater.*, 2005, **53**, 477–485.
8. M. S. Hu and A. G. Evans: *Acta Metall.*, 1989, **37**, 917–925.
9. A. A. Volinsky, N. R. Moody and W. W. Gerberich: *Acta Mater.*, 2002, **50**, 441–466.
10. M. P. K. Turunen, P. Marjamaki, M. Paajanen, J. Lahtinen and J. K. Kivilahti: *Microelectron. Reliab.*, 2004, **44**, 993–1007.
11. J. G. Kohl and I. L. Singer: *Prog. Org. Coat.*, 1999, **36**, 15–20.
12. S. J. Bull and E. G. Berasetegui: *Tribol. Int.*, 2006, **39**, 99–114.
13. N. Ali, Q. H. Fan, J. Gracio and W. Ahmed: *Surf. Eng.*, 2002, **18**, 260–264.
14. M. Larsson, M. Olsson, P. Hedenqvist and S. Hogmark: *Surf. Eng.*, 2000, **16**, 436–444.
15. H. F. Qi, A. Fernandes, E. Pereira and J. Grácio: *Diam. Relat. Mater.*, 1999, **8**, 1549–1554.
16. B. Ekici: *Surf. Eng.*, 2005, **21**, 456–462.
17. G. Marot, J. Lesage, P. Démarécaux, M. Hadad, S. Siegmund and M. H. Staia: *Surf. Coat. Technol.*, 2006, **201**, 2080–2085.
18. J. Lesage and D. Chicot: *Surf. Eng.*, 1999, **15**, 447–453.
19. H. Zhang, Q. Chen and D. Y. Li: *Acta Mater.*, 2004, **52**, 2037–2046.
20. M. D. Bao, X. D. Zhu and J. W. He: *Surf. Eng.*, 2006, **22**, 11–14.
21. B. D. Beake, S. R. Goodes and J. F. Smith: *Surf. Eng.*, 2001, **17**, 187–192.
22. G. Rosa, P. Psyllaki, R. Oltra, T. Montesin, C. Coddet and S. Costil: *Surf. Eng.*, **17**, 332–338.
23. G. Rosa, R. Oltra, C. Coddet, S. Costil and M. H. Nadal: *Surf. Eng.*, 2001, **17**, 472–476.
24. A. A. Ogwu, P. Collieran, P. Maguire, P. Lemoine and J. McLaughlin: *Surf. Eng.*, 2002, **18**, 277–282.
25. J. C. Grosskerutz and M. B. McNeil: *J. Appl. Phys.*, 1969, **40**, 355–359.
26. D. C. Agrawal and R. Raj: *Acta Metall.*, 1989, **37**, 1265–1270.
27. D. C. Agrawal and R. Raj: *Mater. Sci. Eng. A*, 1990, **A126**, 125–131.
28. B. F. Chen, J. Hwang, G. P. Yu and J. H. Huang: *Thin Solid Films*, 1999, **352**, 173–178.
29. F. S. Shieu and M. H. Shiao: *Thin Solid Films*, 1997, **306**, 124–129.
30. A. P. McGuigan, G. A. D. Briggs, V. M. Burlakov, M. Yanaka and Y. Tsukahara: *Thin Solid Films*, 2003, **424**, 219–223.
31. U. Holzwarth and H. Stamm: *J. Nucl. Mater.*, 2002, **300**, 161–177.
32. J. L. Beuth: *Int. J. Solids. Struct.*, 1992, **29**, 1657–1675.
33. J. Dundurs: *J. Appl. Mech.*, 1969, **36**, 650–652.